GEOMETRIC OPTICS MODELLING OF THE POLARIZED BACKSCATTERING FROM A VEGETATION LAYER WITH ROUGH GROUND SURFACE BOUNDARY

Sune R. J. Axelsson

Microwave System Department
Saab-Scania Combitech Group: SMAB
S-581 88 Linköping, Sweden, VII

ABSTRACT

This paper presents the main algorithms of a computer model, which was developed to estimate the polarization characteristics of double-bounce reflection between semi-transparent disc elements and a rough surface below. The polarization matrix of a single disc with arbitrary orientation is first determined. A cloud model is then applied to estimate the backscattering from leaf elements in a canopy. Both single and double bounce reflections from the leaves and the rough soil surface are included. Finally, correlation matrices and probability density functions of the polarized response are derived for two-bounce scattering between dielectric discs and metal surfaces.

Keywords: Radar, scattering, polarization, vegetation.

1. INTRODUCTION

In this paper, the two-bounce and single-bounce scattering from a semi-transparent vegetation canopy is modelled using a geometric optics approach, which can be considered relevant to both mm-waves and optical wavelengths. The model includes as well the interaction between the canopy and the rough ground surface below.

The one-bounce and two-bounce reflections of a single disc object positioned above a rough surface are first analyzed. The single disc model is then generalized to a cloud model containing a large number of discs randomly orientated. Finally, the polarimetric statistics of the scattered wave are analyzed in terms of correlation matrices and probability density functions.

2. POLARIZATION MATRIX OF A TILTED DISC

If n_i is the direction of incidence of the electromagnetic field, the direction of the specular reflection from a tilted disc (n_s) can be expressed as

$$n_s = n_i - 2(n_i n_1)n_1 \qquad (1)$$

where n_1 is the unit normal of the disc satisfying $(n_i n_1) < 0$.

The incident electric field $E_i = E_{vi}v_i + E_{hi}h_i$ and the field reflected by the disc $E_s = E_{vs}v_s + E_{hs}h_s$ are related by the Jones matrix P_d

$$E_s = P_d E_i \qquad (2)$$

The Fresnel reflection coefficients involved are defined assuming that the incident and reflected field components are perpendicular or parallell to the plane of incidence. For that reason, a local coordinate system (n_i, w_i, u_i) has to be introduced as follows

$$u_i = n_1 \times n_i / |n_1 \times n_i| \qquad (3)$$

$$w_i = u_i \times n_i \qquad (4)$$

where u_i is perpendicular to the plane of incidence and w_i is parallel to it.

The polarization directions referred to the external coordinate system (h_i and v_i with h_i in the xy-plane) are also derived from (3) and (4) with $n_1 = z$.

The polarization directions of the reflected wave (h_s, v_s and u_s, w_s) are defined similarly by substituting n_i by n_s.

From (2)-(4), the elements of the polarization matrix of the disc can then be derived as follows

$$P_d(h,h) = (h_i u_i)(u_s h_s)R_u + (h_i w_i)(w_s h_s)R_w \qquad (5)$$

$$P_d(h,v) = (v_i u_i)(u_s h_s)R_u + (v_i w_i)(w_s h_s)R_w \qquad (6)$$

$$P_d(v,h) = (h_i u_i)(u_s v_s)R_u + (h_i w_i)(w_s v_s)R_w \qquad (7)$$

$$P_d(v,v) = (v_i u_i)(u_s v_s)R_u + (v_i w_i)(w_s v_s)R_w \qquad (8)$$

where R_u and R_w are the specular reflection coefficients of the disc.

In (5)-(8), the local unit vectors u and w are used. It is often more useful to express the polarization matrix in terms of n_i and n_s, which define the incidence and scattering directions in the external reference system.

This transformation is straight-forward if an alternative definition of u_i is applied

$$u_i = (n_s \times n_i)/ |n_s \times n_i| \qquad (9)$$

combined with the two vector multiplication rules:

$$A(B \times C) = B(C \times A) \qquad (10)$$

$$A \times (B \times C) = (A C)B - (A B)C \qquad (11)$$

The result is as follows:

$$P_d(h,h) = -[R_w P_1 P_2 + R_u P_3 P_4]/D^2 \qquad (12)$$

$$P_d(h,v) = -[R_w P_1 P_4 - R_u P_2 P_3]/D^2 \qquad (13)$$

$$P_d(v,h) = -[R_w P_2 P_3 - R_u P_1 P_4]/D^2 \qquad (14)$$

$$P_d(v,v) = -[R_w P_3 P_4 + R_u P_1 P_2]/D^2 \qquad (15)$$

where $D = |n_s \times n_i|$, $P_1 = h_s n_i$, $P_2 = h_i n_s$, $P_3 = v_s n_i$ and $P_4 = v_i n_s$ have also been introduced.

3. REFLECTION AND TRANSMISSION COEFFICIENTS

The transmission and reflection coefficients of a flat semi-transparent disc of thickness d and the complex dielectric constant $\epsilon = \epsilon' + j\epsilon''$ can be estimated (Born and Wolf, 1975)

$$R_p = (R_{01} + R_{12}\tau^2)/(1 + \tau^2 R_{01}R_{12}) \qquad (16)$$

$$T_p = \tau T_{01}T_{12}/(1 + \tau^2 R_{01}R_{12}) \qquad (17)$$

where p = u or w, and R_{01}, R_{12}, T_{01}, T_{12} are the Fresnel reflection and transmisssion coefficients of the upper and lower surface boundary of the disc, respectively. The transmission factor τ is determined by

$$\tau = \exp(j\beta) \qquad (18)$$

with

$$\beta = (2\pi d/\lambda)[\epsilon-\sin^2(\theta_0)]^{1/2} \qquad (19)$$

The dielectric constant $\epsilon=4+j4$ is representative for leaves at 95 GHz (Mätzler and Sume, 1989). From (17), it is found that leaves of most species (d = 0.1 - 0.2 mm) have a significant transmission at 95 GHz. For oblique incidence angles, there are also great differences between R_p and T_p for vertical and horizontal polarization as a result of the Brewster angle effect.

As an example, Table 1 shows the phase differences between the parallel and perpendicular polarization components of R_p and T_p for d=0.2 mm, $\lambda=3$ mm and $\epsilon=4+j4$. The phase difference of the transmission coefficients is only a few degrees for most angles of incidence.

TABLE 1. Phase angle difference (degrees) between the reflection coefficients for vertical and horizontal polarization and that of the transmission coefficients (d=0.2 mm, $\lambda=3$ mm and $\epsilon=4+j4$).

INCIDENCE ANGLE	PHASE ANGLE DIFFERENCE	
(Deg.)	Reflection	Transmission
0	-180.0	0.0
30	-176.3	1.0
45	-169.3	2.6
60	-144.1	4.9
75	-55.3	11.7
85	-18.8	28.0

The phase difference of the reflected components is 180 degrees for $\theta_0=0$ but is gradually reduced at oblique incidence (75 and 85 degrees in Table 1). For metal surfaces, however, the 180 degree difference remains for all angles of incidence. This displays the well-known polarization change from right-handed to left-handed rotation (and vice versa) when a circularly polarized wave is reflected by a metal surface. At oblique reflection from a dielectric surface with losses, the scattered wave contains both components.

4. MULTIPLE SCATTERING BETWEEN DISCS

The computation procedure for single reflection can also be extended to multiple scattering between discs with positions and inclinations that make multiple reflections between them possible. The scattering direction of the first reflection then defines the incidence direction of the second one ($n_{i2} = n_{s1}$) and the procedure is repeated. After N reflections, the polarization matrix is defined by

$$P = P_N \ldots P_2 P_1 \qquad (20)$$

By the use of (5)-(20), it is possible to compare the phase difference between the vertical and horizontal components of a two-bounce reflected wave, which is detected by a monostatic radar. The surface normals are assumed to be spherically directed by random but linked together so that the two-bounce reflected wave between two discs is directed back towards the radar receiver. See Figure 1.

For metal discs the phase difference is close to 0 degrees after a two-bounce reflection, because each reflection turns the phase difference about 180 degrees. The two-bounce reflected signal has then approximately the same type of circular polarization as the transmitted (left-handed or right-handed), while the polarization state is reversed for an odd number of reflections.

For dielectric objects with losses, the phase difference is spread out over a much wider angular interval. As a consequence, the two-bounce reflected wave from dielectric objects of random orientation contain both left circular and right circular components, even if the incident wave is right-handed or left-handed polarized.

The reflection between a metal plate and a dielectric disc shows phase difference distributions, which have the same peaks as for double-bounce scattering between two metal discs. The side-lobe level is increased significantly, however.

5. GROUND SURFACE SCATTERING

In order to describe the polarization matrix of two-bounce reflection between a disc and bare ground, the scattering of rough surfaces has to be discussed.

Let us confine the discussion to the situation when the radii of curvature of the surface undulations are of the order of a wavelength or more, which justifies the use of the stationary phase approximation; see Ulaby et al. (1982) and Tsang et al. (1985) for a more detailed discussion.

When the stationary phase condition is satisfied, the surface normal is defined by

$$n_1 = (n_s - n_i)/ |n_s - n_i| \qquad (21)$$

and the elements of of the scattering matrix S can be expressed as

$$S_{pq} = -(jk_0\cos(\theta_{is})/2\pi) \, I \, P_{pq} \qquad (22)$$

where I is the surface integral

$$I = \int \exp(jqr_1)dS_1 \qquad (23)$$

with

$$q = k_0(n_i-n_s) \qquad (24)$$

The angle θ_{is} is the local angle of incidence at the stationary phase points of the ground surface. From (21), it is found that

$$\cos(\theta_{is}) = -n_i n_i = (1-n_i n_s)/ |n_s-n_i| \qquad (25)$$

The matrix element P_{pq} is defined by (12)-(15). However, R_u and R_w now represent the Fresnel reflection coefficients of the ground surface and are defined by its complex dielectric constant.

From Tsang et al. (1985), the correlation products of the scattering matrix elements are then given by

$$<S_{pq}S_{mn}^*> = A \, (k_0q/q_z^2)^2 \cos^2(\theta_{is})p(h_x,h_y)P_{pq}P_{mn}^* \qquad (26)$$

where $p(h_x,h_y)$ is the probability density function of the surface slopes in the x- and y-directions, respectively. The local slopes at the specular points h_x and h_y are obtained from

$$h_x = -q_x/q_z \qquad (27)$$

$$h_y = -q_y/q_z \qquad (28)$$

where q_x, q_y and q_z are defined by (24).

6. DOUBLE-BOUNCE INTERACTION

Let us now consider the scattering from a tilted disc, which is positioned above a rough scattering ground surface. Looking at two-bounce scattering, we notice that there are two different paths of propagation: (i) via the disc and the ground, and (ii) via the ground and the disc, respectively.

For a mono-static radar ($\mathbf{n}_s = -\mathbf{n}_i$), the scattering matrix of the double-bounce reflection can then be written as

$$S = -(jk_0/2\pi)\, I\, \cos(\theta_{is})\, P \qquad (29)$$

where the polarization matrix P is now defined as

$$P = [P_g(\mathbf{n}_{sd}, -\mathbf{n}_i)P_d(\mathbf{n}_i, \mathbf{n}_{sd}) + P_d(-\mathbf{n}_{sd}, -\mathbf{n}_i)P_g(\mathbf{n}_i, -\mathbf{n}_{sd})] \qquad (30)$$

The matrices P_g and P_d are the polarization matrices of the ground and the disc, respectively, and $\mathbf{n}_{sd}$ is the scattering direction of the disc as defined by (1). The principle of reciprocity makes the two matrix products of (30) equal.

The correlation products of S are then from (26)

$$<S_{pq}S_{mn}^*> = A\,(k_0q/q_z^2)^2\,\cos^2(\theta_{is})p(h_x,h_y)P_{pq}P_{mn}^* \qquad (31)$$

where $\mathbf{q}$ is now defined by $\mathbf{q} = k_0(\mathbf{n}_{sd} - \mathbf{n}_s)$ and h_x, h_y by (27)-(28).

The area A in (31) denotes the spot on the ground surface, which is illuminated by the specular reflection via the disc. If the single-sided area of the disc A_0 is introduced, we derive from the geometry

$$A = A_0\,\cos(\theta_{id})/\cos(\theta_{ig}) \qquad (32)$$

where θ_{id} represents the incidence angle of $\mathbf{n}_i$ at the disc and θ_{ig} is the incidence angle of the wave reflected by the disc and propagating towards the ground surface in the direction $\mathbf{n}_{sd}$. Obviously $\cos(\theta_{id}) = -\mathbf{n}_i\mathbf{n}_1$ and $\cos(\theta_{ig}) = -\mathbf{n}_{sd}\mathbf{z}$.

The average radar cross-section of the two-bounce reflection of the disc via the ground and reversely from the ground via the disc is

$$\sigma_{pq} = 4\pi <S_{pq}S_{pq}^*> \qquad (33)$$

Insertion of (31) into (33) gives the radar cross-sections σ_{pq} of the two-bounce reflection of the disc/ground.

An equivalent backscattering radar cross-section per unit area of the disc, representing the double reflection between the disc and the rough surface, is obtained from

$$\sigma^0_{pq} = \sigma_{pq} / A_0 \qquad (34)$$

In the above expressions, the unit normal of the disc was assumed to be fixed. The corresponding relationship for a random unit normal direction is given by

$$<\sigma_{pq}> = \int p(\mathbf{n}_1)\sigma_{pq}(\mathbf{n}_1)\,d\Omega_1 \qquad (35)$$

where $p(\mathbf{n}_1)$ is the probability density function and the integration is performed over 4π.

The above results can be generalized to a cloud of discs. In the mm-wave band, this is a useful model of backscattering from a leaf canopy.

The leaf direction statistics highly depend on the type of vegetation and its state of development. When the leaf normal has a spherical distribution, all directions have the same probability. In that case,

$$p(\mathbf{n}_1) = 1/4\pi \qquad (36)$$

When the mean direction of the leaf normal is horizontal (i.e. vertical leaves in average), we can use, for instance

$$p(\mathbf{n}_1) = (3/8\pi)\,\sin^2(\theta_1) \qquad (37)$$

to model the performance.

An alternative is

$$p(\mathbf{n}_1) = (15/32\pi)\sin^4(\theta_1) \qquad (38)$$

giving a more narrow distribution.

In the case of vertical mean normal direction (i.e. horizontal leaves in average), we can apply

$$p(\mathbf{n}_1) = [(n+2)/8\pi]\,\cos^n(\theta_1/2) \qquad (39)$$

where n is an integer. Figure 2 shows the shapes of $p(\mathbf{n}_1)$ for (36), (38) and (39) for n=4 and n=10.

7. SINGLE BACKSCATTERING FROM VEGETATION

7.1 General model

The leaf area of a vegetation canopy is usually characterized by the leaf-area-index (LAI), which means the total leaf area (one-side) per unit area of the ground. If h is the canopy height, the ratio LAI/h is the leaf area per unit volume.

The radar cross-section per unit area of the ground can be expressed as a sum of three components

$$\sigma^0 = \tau_c\sigma_s^0 + \sigma_v^0 + \sigma_{sv}^0 \qquad (40)$$

where σ_s^0 represents the backscattering of the rough soil-surface, σ_v^0 is the volume scattering from the canopy and σ_{sv}^0 is the scattering due to the interaction between the surface and the canopy elements.

The factor τ_c is the transmission factor of the canopy (two-ways), which can be expressed for mono-static radar as

$$\tau_c = (\tau_e^2 + \tau_0 - 2\tau_0\tau_e) / (1 - \tau_0) \qquad (41)$$

where τ_e is the one-way transmission factor of the vegetation canopy and τ_0 is the corresponding transmission factor when the leaves are considered opaque.

Hence, τ_e and τ_0 can be written as

$$\tau_e = \exp(-k_eh/\cos(\theta_i) \qquad (42)$$

$$\tau_0 = \exp(-k_0h/\cos(\theta_i) \qquad (43)$$

The coefficients k_0 and k_e are given by

$$k_0(\mathbf{n}_i) = (LAI/h)\int |\mathbf{n}_i\mathbf{n}_1|\,p(\mathbf{n}_1)\,d\Omega_1 \qquad (44)$$

$$k_e(\mathbf{n}_i) = (LAI/h)\int |\mathbf{n}_i\mathbf{n}_1|\,[1 - T_1(\mathbf{n}_i,\mathbf{n}_1)]\,p(\mathbf{n}_1)\,d\Omega_1 \qquad (45)$$

where $T_1(\mathbf{n}_i,\mathbf{n}_1)$ is the power transmission factor of the leaf derived from (17) with $T_1 = |T_p|^2$ for p= u or w.

As a consequence of (45), k_e depends on the polarization as well.

For opaque leaves, in particular, $\tau_e = \tau_0$. From (41) follows

$$\tau_c = \tau_0 \qquad (46)$$

For bistatic scattering, the two-paths transmission factor is instead

$$\tau_c(\mathbf{n}_i,\mathbf{n}_s) = \tau_e(\mathbf{n}_i)\tau_e(\mathbf{n}_s) = \exp[-k_eh(1/\cos(\theta_i)+1/\cos(\theta_s)] \qquad (47)$$

which for $\mathbf{n}_s = -\mathbf{n}_i$ (mono-static radar) gives

$$\tau_c(\mathbf{n}_i,-\mathbf{n}_i) = \tau_e^2 \qquad (48)$$

For opaque leaves, the bistatic expression gives in the monostatic limit

$$\tau_c(\mathbf{n}_i,-\mathbf{n}_i) = \tau_0^2 \qquad (49)$$

Comparison between (46) and (49) shows a significant deviation.

This is due to the fact that (47)-(49) are based on the assumption that the positions of the leaf elements in the upward and down-ward paths are statistically independent. This is not true for the monostatic radar, where the same path is used in both directions. For geometric-optics propagation, (41) should therefore be used instead of (48). When $\tau_0 << \tau_e$, however, (41) is approaching (48).

The average radar cross-section of a disc or a leaf can be expressed as follows (Axelsson, 1991)

$$< \sigma_1(\mathbf{n}_i)> = \pi A_0 \rho_0^2 \, [p(\mathbf{n}_i) + p(-\mathbf{n}_i)] \qquad (50)$$

where A_0 is the mean leaf area (one-side) and $\rho_0^2 = |R_p|^2$ is the power reflection coefficient of the leaf according to (16) at perpendicular direction of incidence.

Eq.(50) is a good approximation even when the leaf is slightly curved, provided that the main beam of reflection ($\Delta\Omega_0$) is much smaller than the beam generated by the random distribution of the leaf normal direction.

The volume scattering component σ_v^0 can be estimated, if we first consider a scattering layer of thickness dz at z. The contribution is then given by

$$d\sigma_v^0 = (LAI/hA_0) <\sigma_1(\mathbf{n}_i)> \tau_c(z,\theta_i) \, dz \qquad (51)$$

After integration from z=0 to z=h and use of (50), we obtain

$$\sigma_v^0 = (LAI/h)\pi\rho_0^2 K_2 \int \tau_c(z,\theta_i) \, dz \qquad (52)$$

where $K_2 = p(\mathbf{n}_i) + p(-\mathbf{n}_i)$.

After insertion of (41)-(43) into (52) and series development of the factor $(1-\tau_0)^{-1} = 1+\tau_0+\tau_0^2+\tau_0^3+...$, the following solution of the integral is derived

$$\int \tau_c(z,\theta_i) \, dz = \Sigma \, (I_{1n} + I_{2n} - 2I_{3n}) \qquad (53)$$

where the integration is from 0 to h and the summation from n=0 to infinity.

The terms I_{kn} are defined as follows

$$I_{kn} = [1-\exp(-A_{kn}h/\cos(\theta_i))]\cos(\theta_i)/A_{kn} \qquad (54)$$

where k = 1, 2, 3 and

$$A_{1n} = 2k_e + nk_0 \qquad (55a)$$

$$A_{2n} = (n+1)k_0 \qquad (55b)$$

$$A_{3n} = k_e + (n+1)k_0 \qquad (55c)$$

7.2 Opaque leaves

For opaque leaves, $k_e = k_0$, which means $A_{1n} = A_{2n} = (n+2)k_0$ and $A_{2n} = (n+1)k_0$. Insertion into (53) shows that the sum ends up with the term I_{20}, or

$$\int \tau_c(z,\theta_i)dz = [1-\exp[-k_0h/\cos(\theta_i)]\cos(\theta_i)/k_0 \qquad (56)$$

which can be obtained more directly by integrating (46).

Insertion of (44) and (56) into (52) then yields

$$\sigma_v^0 = \pi\rho_0^2(K_2/K_1)\cos(\theta_i)[1 - \exp(-K_1 LAI/\cos(\theta_i)] \qquad (57)$$

where $K_2 = p(\mathbf{n}_i) + p(-\mathbf{n}_i)$ and

$$K_1 = <|\mathbf{n}_i\mathbf{n}_l|> = \int |\mathbf{n}_i\mathbf{n}_l| \, p(\mathbf{n}_l)d\Omega_l \qquad (58)$$

For non-uniform leaf orientation, the factors K_1 and K_2 introduce a modified dependence on the angle of incidence.

In particular, for spherical distribution of the normal direction $K_1 = <|\mathbf{n}_i\mathbf{n}_l|> = 0.5$ and $K_2 = 1/2\pi$. After insertion into (57) follows

$$\sigma_v^0(\mathbf{n}_i) = \rho_0^2 \cos(\theta_i) \, [1 - \exp(-LAI/(2\cos\theta_i))] \qquad (59)$$

which is displayed in Figure 3.

8. DOUBLE BOUNCE INTERACTION GROUND/LEAVES

The two-bounce radar cross-section of an individual leaf with unit normal $\mathbf{n}_l$ and located at z is

$$\sigma_2(z, \mathbf{n}_i, \mathbf{n}_l) = \sigma_{pq}\tau_1\tau_2\tau_3 \qquad (60)$$

where σ_{pq} is the two-bounce radar cross-section of a single disc according to (30)-(33) and the transmission factors are defined by

$$\tau_k(z, \mathbf{n}_i) = \exp(-k_{ek}r_k) \qquad (61)$$

$$r_1 = (h - z) / \cos(\theta_i) \qquad (62)$$

$$r_2 = z / \cos(\theta_s) \qquad (63)$$

$$r_3 = h / \cos(\theta_i) \qquad (64)$$

In (61), $k_{e1} = k_{e3} = k_e(\mathbf{n}_i)$ and $k_{e2} = k_e(\mathbf{n}_{sd})$, where the unit vector $\mathbf{n}_{sd}$ represents the scattering direction of the leaf according to (1), and $\cos(\theta_s) = -\mathbf{z}\mathbf{n}_{sd}$, where $\mathbf{z}\mathbf{n}_{sd} < 0$ is the condition for reflection towards the ground surface.

The average value of σ_2 with respect to the leaf inclination yields

$$<\sigma_2(z, \mathbf{n}_i, \mathbf{n}_l)> = \tau_1\tau_3<\tau_2 \sigma_{pq}> \qquad (65)$$

The volume-scattering per unit volume is then $N<\sigma_2(z, \mathbf{n}_i, \mathbf{n}_l)>$ i.e.

$$\sigma_{2v}(z, \mathbf{n}_i, \mathbf{n}_l) = [LAI/(hA_0)] <\sigma_2(z, \mathbf{n}_i, \mathbf{n}_l)> \qquad (66)$$

The total two-bounce contribution per unit area ground is obtained by integrating (66) from z=0 to z=h and $\mathbf{n}_l$ over 4π.

$$\sigma_2^0(\mathbf{n}_i) = \int \sigma_{2v}(z, \mathbf{n}_i, \mathbf{n}_l) \, dz = (LAI/hA_0)\int \tau_1\tau_3<\tau_2\sigma_{pq}>dz =$$

$$= (LAI/hA_0)\int \tau_1\tau_3 \int p(\mathbf{n}_l) \, \tau_2 \, \sigma_{pq}(\mathbf{n}_l,\mathbf{n}_i) \, d\Omega_l \, dz \qquad (67)$$

Figure 4 shows as an example the σ_v^0 and σ_2^0 components of a canopy of opaque discs according to Eqs. (59) and (67). The probability density function $p(h_x, h_y)$ of (31) is assumed Gaussian with rms slope m=0.4.

Comparisons between the predictions of Figure 4 and measured data that are available at 95 GHz show a reasonable agreement. In particular, the inclusion of two-bounce scattering makes it possible to explain the cross-polarization response, which usually is about 10 dB below the co-linear ones.

9. DOUBLE BOUNCES BETWEEEN LEAVES

The technique developed above can be extended to the modelling of two-bounce scattering between individual leaf elements. The numerical difficulties will increase, however, because a double integration with respect to z is required.

The leaf canopy is then divided into two thin layers of thickness dz_1 and dz_2. First, the two-bounce scattering between an individual leaf in the layer (z_1, z_1+dz_1) and the leaves in the layer (z_2, z_2+dz_2) are studied similarly as shown by (60)-(64) and (30)-(33). The two-bounce scattering matrix of (30) is modified as follows

$$\mathbf{P} = [\mathbf{P}_d(\mathbf{n}_{sd},-\mathbf{n}_i)\mathbf{P}_d(\mathbf{n}_i,\mathbf{n}_{sd}) + \mathbf{P}_d(-\mathbf{n}_{sd},-\mathbf{n}_i)\mathbf{P}_d(\mathbf{n}_i,-\mathbf{n}_{sd})] \qquad (68)$$

and the illuminated surface A of (31) and (32) is multiplied by a factor $k_e(\mathbf{n}_{sd})dz_2$ adjusting that leaves in a layer of thickness dz_2 cover only a small part of the xy-plane.

The probability density function $p(h_x, h_y)$ of (31) now describes the distribution of leaf slopes and is obtained from $p(\mathbf{n}_l)$.

The transmission distances of (62)-(64) are also modified

$$r_1 = (h-z_1)/\cos(\theta_i) \tag{69}$$

$$r_2 = (z_1-z_2)/\cos(\theta_s) \tag{70}$$

$$r_3 = (h-z_2)/\cos\theta_i \tag{71}$$

The two-bounce contribution from layer (z_2, z_2+dz_2) and the canopy above $(z_1 = z_2$ to $z_1=h)$ is then computed from (61) and (67). The total two-bounce leaf-to-leaf scattering from the whole vegetation layer is finally derived by integration with respect to z_2 (from 0 to h).

10. CORRELATION MATRIX

10.1 Scattering matrix elements

For distributed targets having a large number of subreflectors, of which no one is giving a dominating response, the elements of the instantaneous scattering matrix become random variables with Gaussian distribution and zero means.

For a mono-static radar, the reciprocity relationship $S_{21} = -S_{12}$ can be applied. The polarimetric statistics are then defined by the correlation matrix (3x3)

$$\mathbf{C} = <\mathbf{Y}\,\mathbf{Y}^{*T}> \tag{72}$$

where

$$\mathbf{Y}^T = (S_{11}, S_{12}, S_{22}) \tag{73}$$

Hence, **C** is given by

$$\mathbf{C} = \begin{bmatrix} <|S_{11}|^2> & <S_{11}S_{12}^*> & <S_{11}S_{22}^*> \\ <S_{12}S_{11}^*> & <|S_{12}|^2> & <S_{12}S_{22}^*> \\ <S_{22}S_{11}^*> & <S_{22}S_{12}^*> & <|S_{22}|^2> \end{bmatrix} \tag{74}$$

Computer calculations show that the normalized correlation matrix of double bounce scattering between leaves with spherical leaf normal distribution is given by

$$\mathbf{C} = \begin{bmatrix} 1.0000 & 0.0000 & -0.51+j0.0018 \\ 0.000 & 0.2432 & 0.0000 \\ -0.51-j0.0018 & 0.0000 & 1.0039 \end{bmatrix} \tag{75a}$$

when $\epsilon = 4+j4$, $\lambda = 3$ mm, d = 0.2 mm.

The corresponding correlation matrix of two-bounce reflection between spherically distributed metal discs is

$$\mathbf{C} = \begin{bmatrix} 1.0000 & 0.0000 & 1.0000 \\ 0.0000 & 1.0000 & 0.0000 \\ 1.0000 & 0.0000 & 1.0000 \end{bmatrix} \tag{75b}$$

Let us also compare with the correlation matrix of two-bounce reflection between pairs of metal/dielectric discs

$$\mathbf{C} = \begin{bmatrix} 1.0000 & 0.000 & 0.52+j0.0010 \\ 0.000 & 0.7558 & 0.000 \\ 0.52-j0.0010 & 0.0000 & 1.0034 \end{bmatrix} \tag{75c}$$

A comparison between (75a)-(75c) shows that the three different types of two-bounce reflections are clearly separated from their correlation matrices. They are also different from the specular one-bounce reflection, which for both metal and dielectric surfaces has a correlation matrix given by

$$\mathbf{C} = \begin{bmatrix} 1.0000 & 0.0000 & -1.0000 \\ 0.0000 & 0.0000 & 0.0000 \\ -1.0000 & 0.0000 & 1.0000 \end{bmatrix} \tag{75d}$$

In particular, one-bounce and two-bounce scattering from metallic reflectors are easily separated from the different signs of the element $C(1,3)$. We also have $C(2,2)=0$ (no depolarization) for one-bounce scattering.

It should be denoted that for two-bounce scattering between spherically distributed dielectric discs according to (75a), the element $C(1,3)$ has the same sign as for one-bounce scattering (75d). The reduced correlation between the co-linear responses and the non-zero element $C(2,2)$ of (75a) indicate a significant depolarization, however.

10.2 Combined model

As shown above, the backscattering from vegetation contains both one-bounce and two-bounce components. The combined correlation matrix can be written as a weighted sum of the correlation matrices of the one-bounce and two-bounce scattering ($\mathbf{C}_1$ and $\mathbf{C}_2$) as follows

$$\mathbf{C} = p\mathbf{C}_1 + (1-p)\mathbf{C}_2 \tag{76}$$

where p is the relative amount of the backscattered power generated by one-bounce scattering effects.

Hence, if σ_1^0 denotes the equivalent radar cross-section of the ground due to one-bounce scattering and σ_2^0 that of two-bounce scattering, the weighting factor p is given by

$$p = \sigma_1^0 / (\sigma_1^0 + \sigma_2^0) \tag{77}$$

The matrix $\mathbf{C}_1$ is defined by (75d) and $\mathbf{C}_2$ has to be computed for the particular type of scatterers involved.

As an example, $\mathbf{C}_2$ may be represented by an expression similar to (75a) for a dense vegetation canopy with spherical distribution of the leaf normals.

10.3 Scattered wave

The corresponding variances $\sigma_1^2 = <E_{1s}E_{1s}^*>$ and $\sigma_2^2 = <E_{2s}E_{2s}^*>$ and covariances $\sigma_{12} = <E_{1s}E_{2s}^*>$ of the scattered field components are given by

$$\sigma_1^2 = <(S_{11}E_{1i}+S_{12}E_{2i})(S_{11}E_{1i}+S_{12}E_{2i})^*> = <|S_{11}|^2>|E_{1i}|^2 +$$
$$+ <|S_{12}|^2>|E_{2i}|^2 + 2\text{Re}\{<S_{11}S_{12}^*>E_{1i}E_{2i}^*\} \tag{78}$$

$$\sigma_2^2 = <(S_{21}E_{1i}+S_{22}E_{2i})(S_{21}E_{1i}+S_{22}E_{2i})^*> = <|S_{21}|^2>|E_{1i}|^2 +$$
$$+ <|S_{22}|^2>|E_{2i}|^2 + 2\text{Re}\{<S_{21}S_{22}^*>E_{1i}E_{2i}^*\} \tag{79}$$

726

$$\sigma_{12} = <(S_{11}E_{1i}+S_{12}E_{2i})(S_{21}E_{1i}+S_{22}E_{2i})^*> =$$

$$= <S_{11}S_{21}^*>|E_{1i}|^2 + <S_{12}S_{22}^*>|E_{2i}|^2$$

$$+ <S_{11}S_{22}^*>E_{1i}E_{2i}^* + <S_{12}S_{21}^*>E_{2i}E_{1i}^* \qquad (80)$$

where E_{1i} and E_{2i} are defined by the polarization state of the incident wave.

The complex correlation coefficient between the two components of the scattered field is obtained from

$$\rho_c = \rho - j\mu = \sigma_{12}/\sigma_1\sigma_2 \qquad (81)$$

where

$$\rho = Re\{\sigma_{12}/\sigma_1\sigma_2\} \qquad (82)$$

$$\mu = -Im\{\sigma_{12}/\sigma_1\sigma_2\} \qquad (83)$$

11. PROBABILITY DENSITY FUNCTIONS

The scattered field $\mathbf{E}_s = (E_{1s}, E_{2s})$ can be expressed in real and imaginary parts as follows: $E_{1s} = X_1 + jY_1$ and $E_{2s} = X_2 + jY_2$.

The probability density function of the scattered field components (X_1, X_2, Y_1, Y_2) is then

$$p(X_1,X_2,Y_1,Y_2) = (1/4\pi^2D^2)exp\{-(1/2D^2)[\sigma_2^2(X_1^2+Y_1^2)+$$

$$\sigma_1^2(X_2^2+Y_2^2)-2\rho\sigma_1\sigma_2(X_1X_2+Y_1Y_2)-2\mu\sigma_1\sigma_2(X_1Y_2-Y_1X_2)]\} \quad (84)$$

where

$$D^2 = \sigma_1^2\sigma_2^2(1-\rho^2-\mu^2) \qquad (85)$$

The parameters σ_1, σ_2, ρ and μ can be expressed in terms of the scattering matrix elements and the incident wave according to (78)-(83).

As an alternative, E_{1s} and E_{2s} can be expressed in polar form

$$E_{1s} = r_1exp(j\theta_1) \qquad (86)$$

$$E_{2s} = r_2exp(j\theta_2) \qquad (87)$$

The probability density function $p_1(r_1,r_2,\theta_1,\theta_2)$ is then derived from

$$p_1(r_1,r_2,\theta_1,\theta_2)dr_1dr_2d\theta_1d\theta_2 = p(X_1,X_2,Y_1,Y_2)dX_1dX_2dY_1dY_2 \quad (88)$$

After introducing the Jacobian determinant, we derive

$$p_1(r_1,r_2,\theta_1,\theta_2) = (r_1r_2/4\pi^2D^2)exp\{-(1/2D^2)[\sigma_2^2r_1^2 + \sigma_1^2r_2^2 -$$

$$- 2\rho\sigma_1\sigma_2r_1r_2cos(\theta_1-\theta_2) + 2\mu\sigma_1\sigma_2r_1r_2sin(\theta_1-\theta_2)]\} \quad (89)$$

Substitution of $\Delta\theta = \theta_1-\theta_2$ and integration with respect to θ_2 from 0 to 2π give as a result the following probability density function of the envelopes and phase difference of the scattered polarization components

$$p_2(r_1,r_2,\Delta\theta) = (r_1r_2/2\pi D^2)exp\{-(1/2D^2)[\sigma_2^2r_1^2 + \sigma_1^2r_2^2 -$$

$$- 2\rho\sigma_1\sigma_2r_1r_2cos(\Delta\theta) + 2\mu\sigma_1\sigma_2r_1r_2sin(\Delta\theta)]\} \quad (90)$$

The polarization ellipse is defined by its rotation and ellipticity angle ψ and χ, respectively. The polarization characteristics can be nicely described using the Poincare' sphere, where 2χ is the latitude and 2ψ is the longitude; see Ulaby and Elachi (1990).

Linear polarization is mapped on the equator of the sphere ($2\chi=0$) with $2\psi=0$ and π corresponding to vertical and horizontal polarization, respectively. Circular polarization is represented by $2\chi = \pi/2$ (left-handed) and $-\pi/2$ (right-handed) i.e. the two poles.

The rotation and ellipticity angles fluctuate strongly as a result of the randomness of the scattered wave. After introducing the ratio $y=\sigma_1/\sigma_2$, the average values of the rotation and ellipticity angles ψ_m and χ_m can be expressed as

$$sin(2\chi_m) = -2\mu y/[(y^2+1)^2 - 4y^2(1-\rho^2-\mu^2)]^{1/2} \qquad (91)$$

$$cos(2\psi_m) = (y^2-1)/\{cos(2\chi_m)[(y^2+1)^2-4y^2(1-\rho^2-\mu^2)]^{1/2}\} \quad (92)$$

$$sin(2\psi_m) = 2\rho y/\{cos(2\chi_m)[(y^2+1)^2-4y^2(1-\rho^2-\mu^2)]^{1/2}\} \quad (93)$$

and the fluctuations of ψ and χ are described by the probability density function $p(\psi,\chi)$ as follows (Axelsson, 1992)

$$p(\psi,\chi) = T(\psi,\chi) / N(\psi,\chi) \qquad (94)$$

where $T(\psi,\chi)$ and $N(\psi,\chi)$ are defined as

$$T(\psi,\chi) = 4(1-\rho^2-\mu^2)|cos(2\chi)| \qquad (95)$$

$$N(\psi,\chi) = \pi\{(y+1/y)+(1/y-y)cos(2\psi)cos(2\chi)$$

$$-2[\rho sin(2\psi)cos(2\chi)-\mu sin(2\chi)]\}^2 \qquad (96)$$

For $\sigma_1 = \sigma_2$ or $y=1$, it is found from (94)-(96) that $p(\psi,\chi)$ depends solely on χ. This case occurs for circular polarized waves.

Figure 5 shows some representative graphs of $p(\psi,\chi)$ for double bounce-scattering betweeen leaves for different polarizations of the incident wave. The corresponding responses from two-bounce scattering between pairs of metallic/dielectric discs are shown in Figure 6.

Figure 7 displays $p(\psi,\chi)$ of the combined response from one-bounce and two-bounce reflections as defined by (75d), (75a) and (76)-(77) for $\sigma_1^0=4\sigma_2^0$, which means dominating one-bounce scattering ($p=0.8$).

At the interpretation of the graphs, we should notice that one-bounce scattering gives strong peaks at the following angles:

a) $E_i=(1,0)$, vertical polarization: $2\psi = 0$, $2\chi = 0$

b) $E_i=(0,1)$, horizontal polarization: $2\psi = \pi$, $2\chi = 0$

c) $E_i=(1,j)$, circular right-handed polarization, gives left-handed polarization as response: $2\chi = \pi/2$.

The corresponding two-bounce responses from metallic discs are given by:

a) $E_i=(1,0)$ i.e. vertical polarization: $2\psi = 0$, $2\chi = 0$

b) $E_i=(0,1)$ i.e. horizontal polarization: $2\psi = \pi$, $2\chi = 0$

c) $E_i=(1,j)$ i.e. circular right-handed polarization gives also right-handed polarization as response: $2\chi = -\pi/2$.

As shown by the graphs, there are significant differences in the polarization response $p(\psi,\chi)$ for all the three cases. For circular right-handed polarization, the position of the ridge along the χ-axis is a good indicator of the type of reflection. Hence, the metal/dielectric disc combination of Figure 6 shows a negative χ-angle, the dominating one-bounce reflection of Figure 7 gives a positive χ-angle, while the two-bounce reflections from dielectric discs (Figure 5) fall between.

727

REFERENCES

Axelsson, S.R.J., 1991. Polarization dependence of two-bounce scattering from disc objects located above a rough ground surface. Proc. 24th Symp.Rem.Sens. Environm., Rio de Janeiro, 27-31 May 1991.

Axelsson, S.R.J., 1992. Polarimetric statistics of electromagnetic waves scattered by distributed targets. Swedish Defence Research Establishment, Linköping, Technical Report C 30656-3.3, ISSN 0347-3708.

Born, M. and E. Wolf, 1975. Principles of Optics. Pergamon Press, Fifth Edition, Oxford.

Mätzler, C. and A. Sume, 1989. Microwave radiometry of leaves. Proceedings of the specialist meeting on microwave radiometry and Remote Sensing applications, Florence, Italy, March 1988.

Tsang, L., J.A. Kong and R.T. Shin, 1985. Theory of Microwave Remote Sensing. Wiley-Interscience, New York.

Ulaby, F.T., R.K. Moore and A.K. Fung, 1982. Microwave Remote Sensing. Addison-Wesley Publ. Co., London.

Ulaby, F.T., and C. Elachi, 1990. Radar Polarimetry for Geoscience Applications. Artech House, Norwood.

PROBABILITY DENSITY FUNCTIONS OF DISC NORMAL DIRECTION

A. Isotropic

B. $p(n_l) = [3/4\pi]\cos^4(\theta_l)$

C. $p(n_l) = [3/2\pi]\cos^{10}(\theta_l)$

D. $p(n_l) = (15/32\pi)\sin^4(\theta_l)$
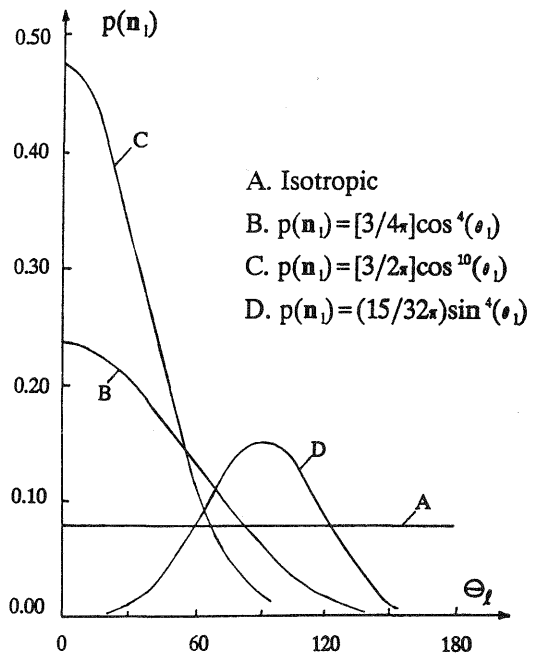
Figure 2. Examples of probability density functions of the leaf normal direction $p(n_l)$.

Figure 1. Predicted distributions of the phase angle difference $\phi_{VV}-\phi_{HH}$ between the two-bounce reflection coefficients (S_{VV} and S_{HH}) when the incident wave is scattered by a cloud of discs with spherical distribution of the normal directions ($\epsilon = 4+j4$, $\lambda = 3$ mm, $d = 0.2$ mm).

VOLUME BACKSCATTERING FROM A CLOUD OF OPAQUE DISCS (HH AND VV).
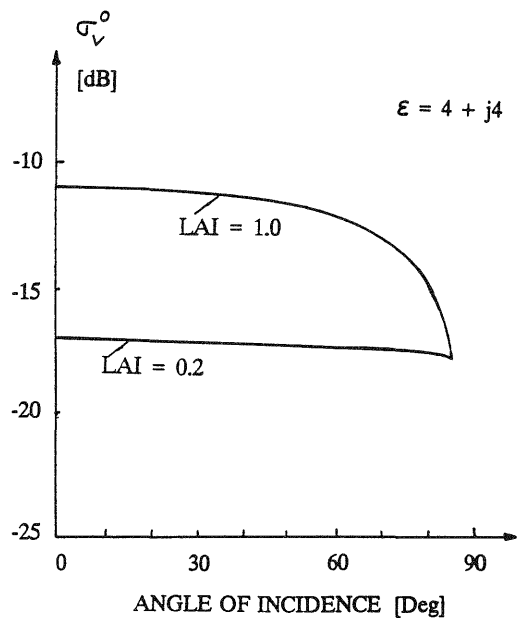
Figure 3. Single-bounce volume backscattering (VV and HH) from opaque spherically distributed leaves ($\epsilon = 4+j4$).

728
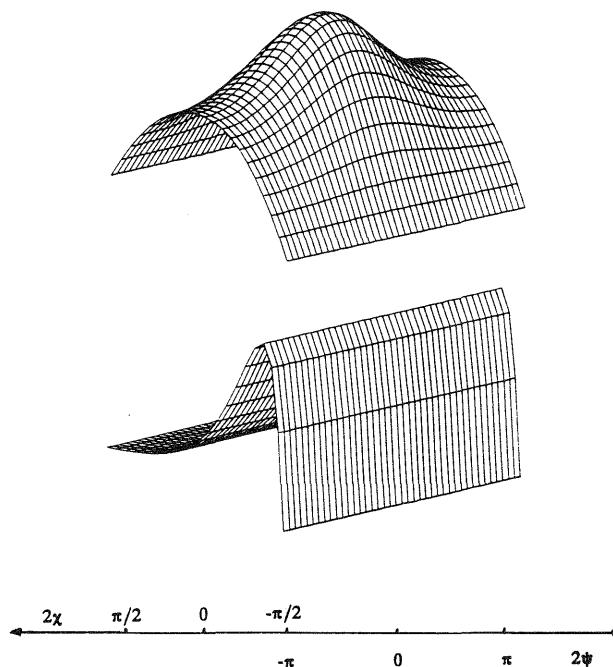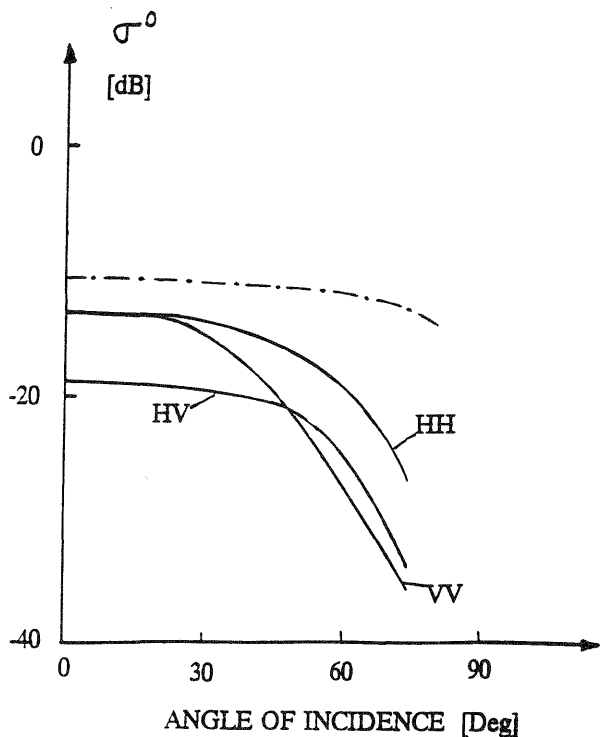
Figure 4. Two-bounce backscattering components between spherically distributed opaque leaves and the ground surface. Single-bounce backscattering from the leaves is dashed. Computed from Eqs.(59) and (67) with LAI = 1, h = 1 m, m = 0.4 and $\epsilon_g = \epsilon_1 = 4 + j4$.

Figure 6. The probability density function $p(\psi, \chi)$ for double-bounce scattering between pairs of metallic and dielectric discs with spherical distribution ($\epsilon = 4 + j4$, $\lambda = 3$ mm, d = 0.2 mm). Vertical polarization (top) and right-handed circular (below).
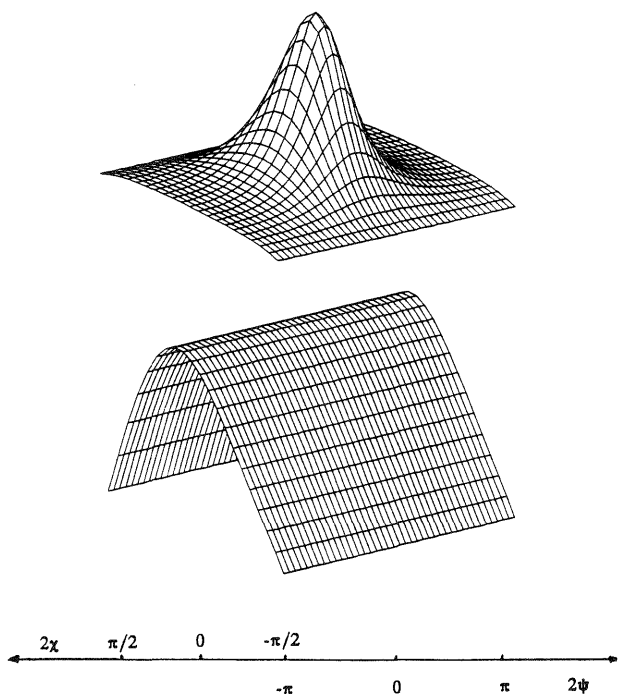
Figure 5. The probability density function $p(\psi, \chi)$ for double-bounce scattering between leaves with spherical distribution ($\epsilon = 4 + j4$, $\lambda = 3$ mm, d = 0.2 mm). Vertical polarization (top) and right-handed circular (below).
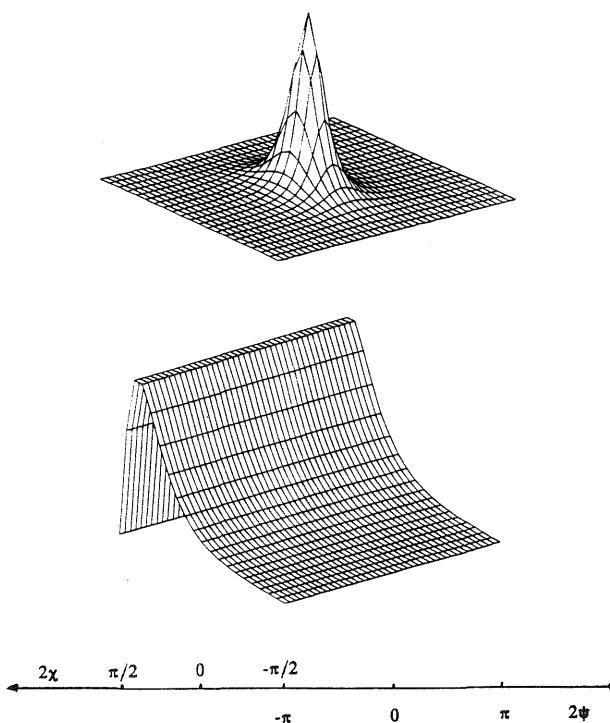
Figure 7. The probability density function $p(\psi, \chi)$ of the combined response from one-bounce and two-bounce reflections as defined by (75d), (75a) and (76)-(77) for $\sigma_1^0 = 4\sigma_2^0$ (one-bounce scattering dominates). Vertical polarization (top) and right-handed circular (below).